

**The Inclusion of Salinity in a Simple
Steady-State Coupled Ice-Ocean Model
of the Greenland-Norwegian Sea**

**Paul G. Myers, Jianping Gan
and Marie Robert
C²GCR Report No. 92-9
June 1992**

The Inclusion of Salinity in a Simple Steady-State Coupled Ice-Ocean Model of the Greenland-Norwegian Sea

Paul G. Myers, Jianping Gan and Marie Robert

Department of Atmospheric and Oceanic Sciences
and
Centre for Climate and Global Change Research
McGill University
805 Sherbrooke St. West
Montreal, P.Q., H3A 2K6
Canada

Abstract

The steady, coupled ice-ocean circulation model of Willmott and Mysak (1989) is modified to allow for horizontal variations in the upper level salinity field. The model is then applied to the Greenland and Norwegian Seas, between 60° and 80°N, and between the east coast of Greenland and 15°E. The model gives a reasonable simulation of the observed climatological surface salinity field in the region. The surface density field is then calculated and likely regions of convective overturning are identified.

1.0 Introduction

The main connection between the Arctic and Atlantic Oceans is through Fram Strait and the Greenland-Norwegian Seas. Warm North Atlantic water enters the Arctic at intermediate depths along the eastern side of Fram Strait while cold water and ice exit the Arctic along the east coast of Greenland in the East Greenland Current (EGC) (Muench et al.,1992). Through this export of fresh water, the Arctic Ocean controls the ocean ventilation in the Greenland and Iceland Seas (Aagaard & Carmack,1989). The mechanism by which this control is exerted is by the release of fresh water from the boundary current into the interior of the convective gyres (Aagaard & Carmack,1989). The Greenland-Norwegian Seas include some of the most important locations for the formation of North Atlantic Deep Water (NADW) (Gordon,1986), which plays a key role in the large-scale thermohaline circulation.

For these reasons, there has been, and still is, strong interest in studying the Greenland-Norwegian Seas region. Numerous field studies have been conducted to study the current structure and water mass properties of the region (e.g. Quadfasel & Meincke,1987; van Aken et al.,1991; Muench et al.,1992). A number of coupled ice-ocean modelling studies have been performed as well. The latter include simulations of the ice edge of this region, and model studies of other high latitude ice-ocean processes that are applicable to these two seas.

In general, the modelling studies generally fall into one of three types: (i) Large-scale, three-dimensional ocean general circulation models that are coupled to sophisticated dynamic and thermodynamic sea-ice models (e.g. Hibler & Bryan,1984 1987; Semtner,1987; Holland et al.,1992); (ii) Mesoscale wind-driven models of the marginal ice zone that use highly idealized ice-edge geometry and simplified ice and ocean dynamics (e.g. Røed &

O'Brien,1983; Ikeda,1985; Hakkinen, 1986 1987); (iii) Coupled one-dimensional mixed-layer thermodynamic sea-ice models (e.g. Røed,1984; Fichefet & Gaspar,1988).

Recently, Willmott and Mysak (1989, hereafter referred to as WM) developed a relatively simple model intermediate in complexity and scale between the first two categories listed above. It is a steady state model that couples a wind-driven thermodynamic reduced-gravity ocean to a continuous, thermal equilibrium ice sheet that extends across a meridional channel. Despite some limitations due to its simplicity, the model simulates the annual climatological temperature field and ice-edge configuration for the Greenland-Norwegian Seas quite well. Since the initial work of WM, the model has been successfully used to model the winter ice-edge position in the northern portion of the Labrador Sea (Mysak et al.,1991). Furthermore, an extended version of the model, including a southward flowing buoyancy-driven current and improved lateral mixing has been developed (Wood & Mysak,1989).

A major shortcoming of the original WM model was that upper level salinity was kept constant throughout the analysis. In the version of the model presented here, we allow the salinity to vary with precipitation and evaporation. By adding salinity, we calculate the upper layer density field and hence determine its spatial variations. From this field, the potential regions of convective overturning can be found.

The outline of this paper is as follows. In section 2, the changes that we make to the WM model are discussed. The results of these modifications are presented in section 3, while the significance of the results are discussed in section 4.

2.0 The Model

We use an extension of the Willmott and Mysak (1989) model to study the climatological upper ocean salinity structure of the Greenland-Norwegian Seas between 60° and 80°N. This region is represented as a meridional channel on a beta plane. Our coordinate system and domain boundaries are defined to be the same as WM.

The oceanic model consists of a 2-layer thermodynamic reduced-gravity model (see Fig. 3 of WM). In the upper active layer, temperature $T_1(x,y)$, salinity $S_1(x,y)$ and velocity $\mathbf{v}_1(x,y)$ are allowed to vary horizontally. It is assumed that in this steady-state model the basic stratification is stable, i.e., $\rho_0 - \rho_1 > 0$ (where $\rho_0(T_0, S_0)$ and $\rho_1(T_1, S_1)$ are the densities of the lower and upper levels, respectively). The process of convective overturning would then consist of time-dependant perturbations on this state.

The volume transport streamfunction, Ψ , is determined using the Sverdrup equation (see eq. (2.10) of WM), for regions south of the ice edge and outside of the western boundary current. We use the simple "Stommel-type" frictional boundary current of WM in the western boundary layer to close the circulation. We do not use the extended model version of Wood and Mysak (1989) that includes a buoyancy-driven western boundary current due to the increased numerical requirements it involves.

The upper ocean temperature and salinity satisfy the horizontal advection equations

$$hu_1T_{1x} + hv_1T_{1y} = Q_0 \quad (2.1)$$

$$hu_1S_{1x} + hv_1S_{1y} = B_0 \quad (2.2)$$

where h is the depth of the upper layer, $\mathbf{v}_1=(u_1, v_1)$ is the depth independent horizontal velocity in the upper layer, and Q_0 and B_0

are the surface sources and sinks of heat and salinity. The temperature equation is forced by a Haney-type heat flux (see eq. (2.11) in WM).

Unlike WM, we do not set $B_o = 0$, and so allow the upper-layer salinity S_1 to vary horizontally over the domain. This is an important addition as it is vital to retain salinity in the equation of state at high latitudes (Bryan,1986). We force the salinity equation (2.2) by a salt flux into the ocean

$$B_o = c_1 (E - P) \quad (2.3)$$

where $(E - P)$ is the observed evaporation minus precipitation field, in metres per year. The dimensionless proportionality constant c_1 is determined experimentally.

Both of these advection equations (temperature and salinity) are first-order partial differential equations whose characteristics are given by transport streamlines. Thus they can be solved by integrating poleward along the characteristics that emanate from the southern boundary, $y = -y_0$. Here, as in WM, $y_0 = L$ is the channel width.

To do this, the temperature and salinity fields have to be specified along the southern boundary. These are $T_1(x, -y_0)$ and $S_1(x, -y_0)$, respectively. For temperature, we use the analytical expression of WM, while for salinity we use data composited from Levitus (1982).

We use the ice model of WM with no modifications. That is, it is treated as a stationary, conducting slab of thickness $d(x,y)$. It is affected by heat fluxes to and from the ocean and the atmosphere.

3.0 Results

All forcing fields except for the (E - P) field, which was not included in the WM model, are exactly as in WM. We use the (E - P) data compiled by Schmitt et al. (1989). This (E - P) field is shown in Figure 1. Note that the accuracy of this data, especially in high latitude regions, such as the one that we are looking at, is not good (Schmitt et al., 1989). The parameters we use are basically those of WM. For those variables which WM vary over the course of several experiments, we assume the following values: the distance the wind stress is shifted southward from the origin, $d = 0$; the windstress τ is rotated counterclockwise $\theta = 45^\circ$ from the positive x-axis; and the air-sea exchange coefficients for heat is $k_{aw} = 25 \text{ W m}^{-2} \text{ K}^{-1}$ (see WM for an explanation of the choice of this parameter). The vertical exchange coefficients for heat flow between the ice-ocean, k_{iw} , and air-ice, k_{ai} , interfaces are set, respectively, to $6 \text{ W m}^{-2} \text{ K}^{-1}$ and $8 \text{ W m}^{-2} \text{ K}^{-1}$, which are slightly different than in WM.

Using these values we reproduce the ice edge (Fig. 2) and upper level temperature fields (see Fig. 11 of WM) of WM. Then using the same streamfunction field, we solve the salinity advection equation using the method of characteristics. The coefficient c_1 from (2.1) is used as a tuning parameter. We find that a value of $2 * 10^{-6}$ for c_1 gives us a salinity field that is in close agreement with the salinity field composited from the atlas of Levitus (1982) (Fig. 3).

Our calculated upper ocean salinity field is shown in Figure 4. It reproduces the observed surface salinity field (Fig. 3) quite well, at least in a qualitative sense. The main feature in this region, the long extended tongue of water with salinity greater than 35.0 is reasonably reproduced. Our model does not reproduce the wedge of fresh water extending down the western boundary, but

this is to be expected as our model does not include the strong equatorward transport of fresh water by the EGC. As well, there is a discrepancy in the southeast corner of the domain, due to the presence of land (Scandinavia), which we have not included in our model experiments.

We now use these temperature and salinity fields to determine the upper ocean density field for the Greenland-Norwegian Seas. We use the full non-linear equation of state, taken from Gill (1982). This produces the density field shown in Figure 5. The density is maximum in the northern part of the 35.0 salinity region. The density is least along the eastern edge of the domain due to the lower salinities there and because of the warm tongue of North Atlantic water stretching poleward in that region.

4.0 Discussion and Summary

We have taken the simple coupled ice-ocean model of WM and have added variable upper layer salinity. We were able to produce a reasonable reproduction of the observed surface salinity field in the Greenland-Norwegian Seas. The general salinity features of the region were simulated except for the freshening along the Greenland coast, due to the advection of fresh water and ice from the Arctic by the EGC. The reason for this discrepancy is the lack of a western boundary current in our model.

Our model does not include the effects of the melting and freezing of ice on density. During ice formation, the ocean salinity increases due to brine rejection while it decreases when ice melts. However, since our model is a steady-state one, freezing and melting will be in balance, and so in this they can be assumed to have an equal effect on the salinity field, and hence can be ignored in this simple approach.

Being able to simply reproduce a reasonably accurate picture of the upper ocean salinity field is of value due to the importance of salinity on the density field at low temperatures (Weyl, 1968). This is important because the density field governs the ocean's stratification, and the stability of this stratification should indicate regions where convective overturning may occur.

Although we have assumed that convection cannot occur in our model (the model always has stable stratification), we can hypothesize it is likely to occur where the density differences between the upper and lower levels is least. The density difference between the two levels is shown in Figure 6. This shows that overturning is most likely to occur in the northern and western parts of the domain where the salinity is the greatest and temperatures are the coldest. The small region of negative density difference near the western boundary (Fig. 6) is due to a breakdown

of our basic assumption of static stability. However, this is not a concern, because in reality the surface density at this location will be much lower due to the effects of the EGC, as discussed below.

The reduction in surface density along the western coast of Greenland is due to effects of the EGC and its strong freshwater transport equatorward down the coast. This indicates a region in the north central part of the domain where convection is most likely to occur. This corresponds roughly with the centre of the Greenland Sea gyre, which is where convection is generally thought to occur (e.g. van Aken et al., 1991). Note that we are using annually averaged forcing fields, while convection is believed to occur mainly in winter, when the water column can be further cooled by the atmosphere. This lack of winter cooling may help explain why we see no region of possible convective overturning farther south in the Norwegian Sea gyre.

In conclusion, adding salinity in the simple WM model of gives a simple and reasonably accurate way to simulate surface salinity in high latitude regions near a climatological ice edge. From this, regions of likely convective overturning can be suggested. This model gives us a rapid and inexpensive tool that can be used to locate possible regions of convective activity for further study in more realistic, but more costly and complex models.

Acknowledgements

We would like to thank Dr. Lawrence Mysak for proposing this project, which was part of the requirements for a departmental graduate level course in Arctic Oceanography and Climate. We would also like to thank Dr. Mysak and Dr. Grant Ingram for their helpful advice. We would also like to thank Dr. Andrew Weaver for providing us with the E - P data which we used.

References

- Aagaard, K. and E.C. Carmack, 1989: The role of sea ice and other fresh water in the Arctic Circulation, *Journal of Geophysical Research*, **94**, 14485-14498
- Fichefet, T. and P. Gaspar, 1988: A model study of upper ocean-sea ice interactions, *Journal of Physical Oceanography*, **18**, 181-195
- Gill, A.E., 1982: "Atmosphere-Ocean Dynamics", Academic Press, London
- Gordon, A.L., 1986: Interocean exchange of thermocline water, *Journal of Geophysical Research*, **91**, 5037-5046
- Hakkinen, S., 1986: Ice banding as a response of the coupled ice-ocean system to temporally varying winds, *Journal of Geophysical Research*, **91**, 5047-5053
- Hakkinen, S., 1987: Feedback between ice flow, barotropic flow and baroclinic flow in the presence of bottom topography, *Journal of Geophysical Research*, **92**, 3807-3820
- Hibler III, W.D. and K. Bryan, 1984: Ocean circulation. Its effect on seasonal sea-ice simulations, *Science*, **224**, 489-492
- Hibler III, W.D. and K. Bryan, 1987: A diagnostic ice-ocean model, *Journal of Physical Oceanography*, **17**, 987-1015
- Holland, D.M., L.A. Mysak, D.K. Manak and J.M. Oberhuber, 1992: Simulation of the seasonal Arctic sea-ice cover with a dynamic thermodynamic sea-ice model, submitted to *Journal of Geophysical Research*
- Ikeda, M., 1982: A coupled ice-ocean model of a wind-driven coastal flow, *Journal of Geophysical Research*, **90**, 9119-9128
- Levitus, S., 1982: Climatological atlas of the world ocean, NOAA professional paper 13, U.S. Department of Commerce: National Oceanic and Atmospheric Administration
- Muench, R.D., M.G. McPhee, C.A. Paulson and J.H. Morison, 1982: Winter oceanographic conditions in the Fram Strait-Yermak Plateau Region, *Journal of Geophysical Research*, **97**, 3469-3483
- Mysak, L.A., S. Peng and R.G. Wood, 1991: Application of a coupled ice-ocean model to the Labrador Sea, *Atmosphere-Ocean*, **29**, 232-255
- Quadfasel, D. and J. Meincke, 1987: On the thermal structure of the Greenland Sea gyres, *Deep-Sea Research*, **34**, 1883-1888
- Røed, L.P., 1984: A thermodynamic coupled ice-ocean model of the marginal ice zone, *Journal of Physical Oceanography*, **14**, 1921-1929
- Røed, L.P. and J.J. O'Brien, 1983: A coupled ice-ocean model of upwelling in the marginal ice zone, *Journal of Geophysical Research*, **88**, 2863-2872
- Schmitt, R.W., P.S. Bogden and C.E. Dorman, 1989: Evaporation minus precipitation and density fluxes for the North Atlantic,

Journal of Physical Oceanography, **19**, 1208-1221

van Aken, H.M., D. Quadfasel and A. Warpakowski, 1991: The Arctic front in the Greenland Sea during February 1989: Hydrographic and biological observations, *Journal of Geophysical Research*, **96**, 4739-4750

Weyl, P.K., 1968: The role of the oceans in climatic change. A theory of the ice ages, *Meteorological Monographs*, **8**, 37-62

Willmott, A.J. and L.A. Mysak, 1989: A simple steady-state coupled ice-ocean model, with applications to the Greenland-Norwegian Sea, *Journal of Physical Oceanography*, **19**, 501-518

Wood, R.G. and L.A. Mysak, 1989: A simple ice-ocean model for the Greenland Sea, *Journal of Physical Oceanography*, **19**, 1865-1880

Figure Captions

- Figure 1.** Annual mean evaporation minus precipitation field, in metres per year, from Schmitt et al. (1989).
- Figure 2.** The ice edge curve for $q=0.75$ and $k_{aw} = 25 \text{ W m}^{-2} \text{ K}^{-1}$.
- Figure 3.** A composite of the observed surface salinity field, taken from Levitus (1982).
- Figure 4.** The upper ocean salinity field as produced by the model. Contour interval is 0.5.
- Figure 5.** The upper ocean density field of the region produced using the model's temperature and salinity fields. Contour interval is 0.25.
- figure 6.** Density difference between the fixed lower level density field ($\rho_0 = 1028 \text{ kg m}^{-3}$) and the predicted upper level density, as shown in figure 5. Contour interval is 0.09.

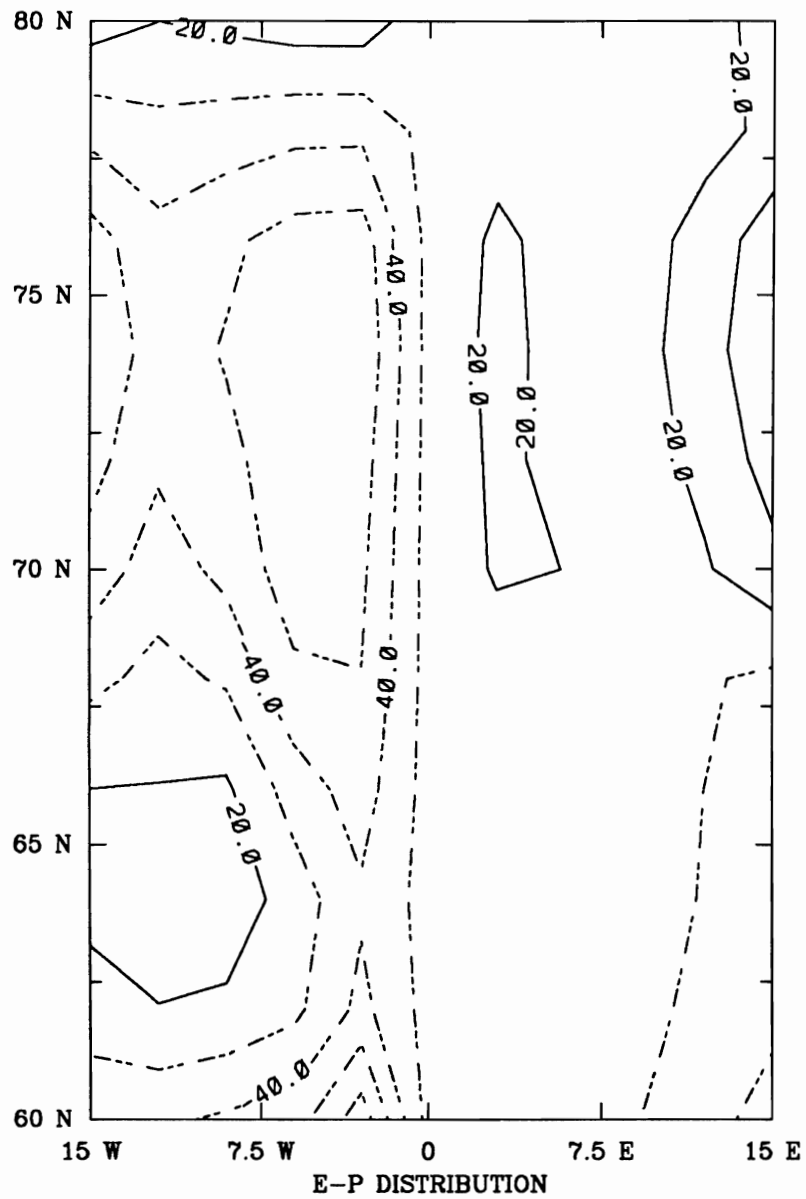


Figure 1. Annual mean evaporation minus precipitation field, in metres per year, from Schmitt et al. (1989).

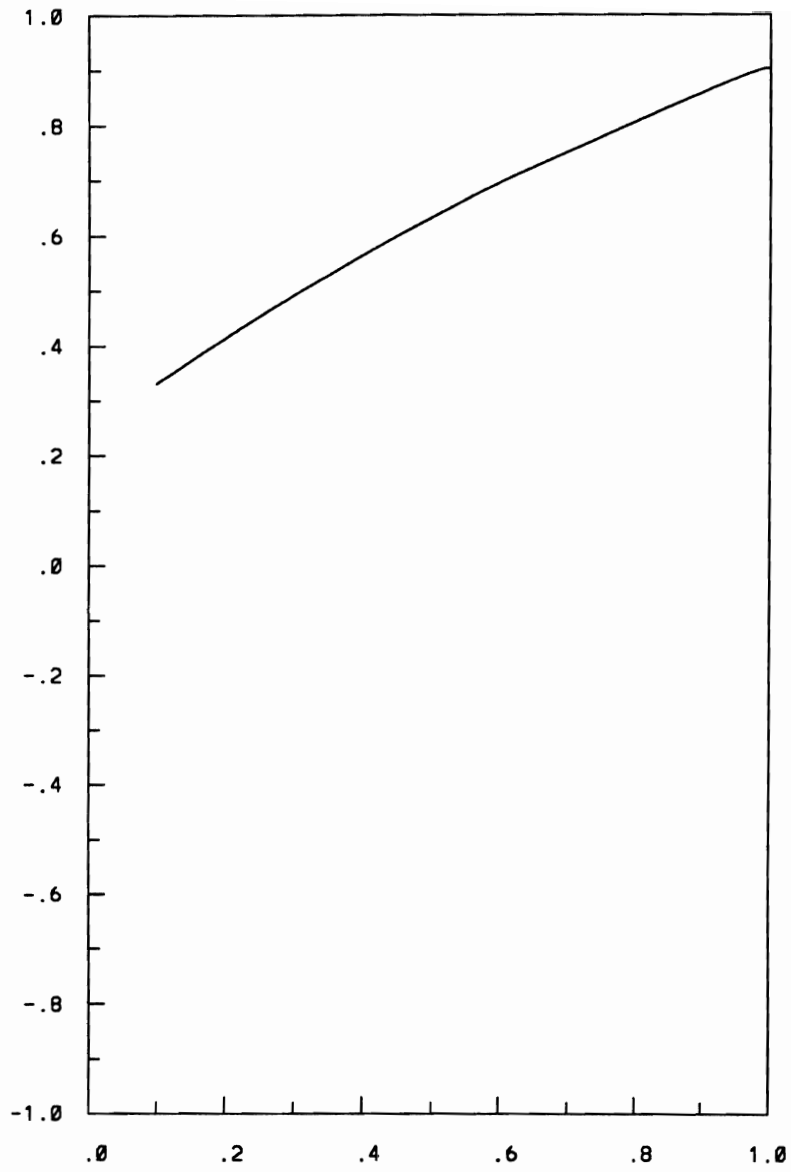


Figure 2. The ice edge curve for $q=0.75$ and $k_{aw} = 25 \text{ W m}^{-2} \text{ K}^{-1}$.

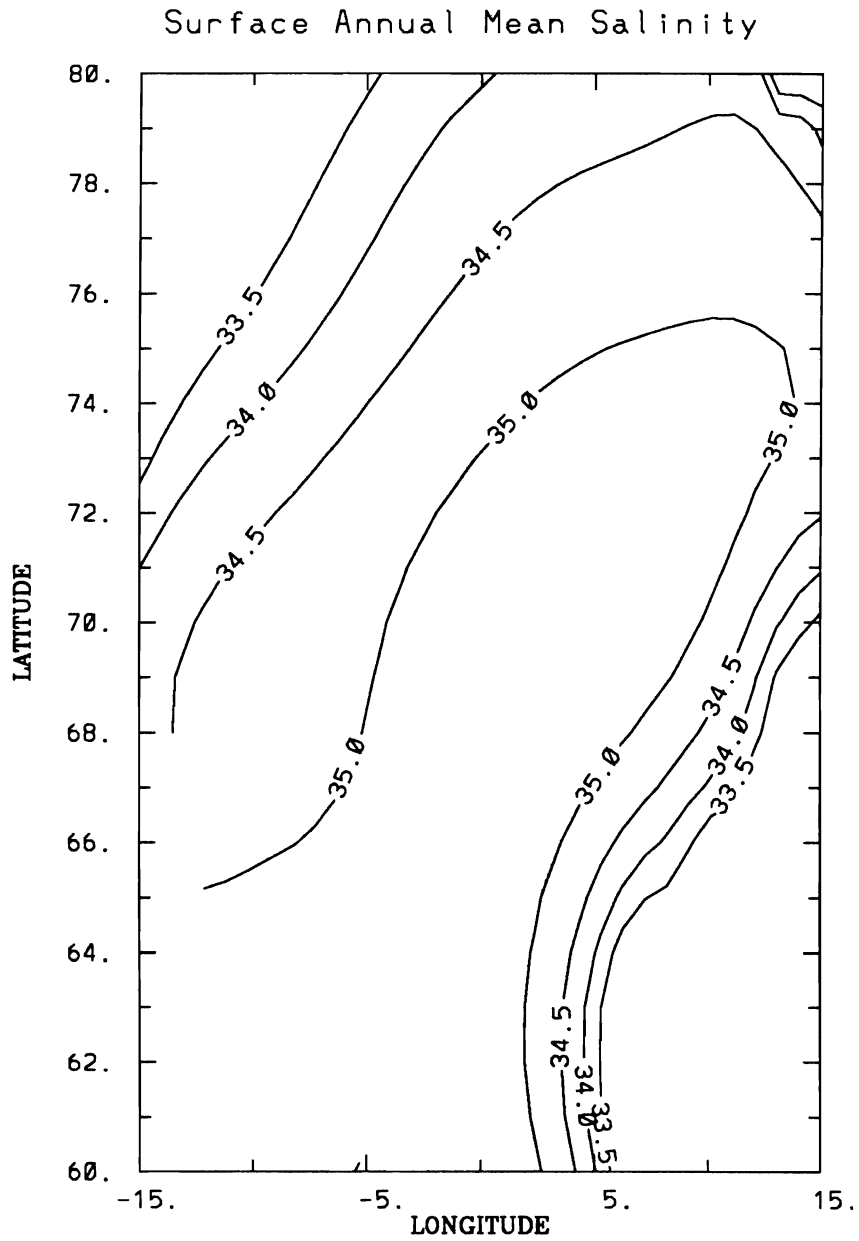


Figure 3. A composite of the observed surface salinity field, taken from Levitus (1982).

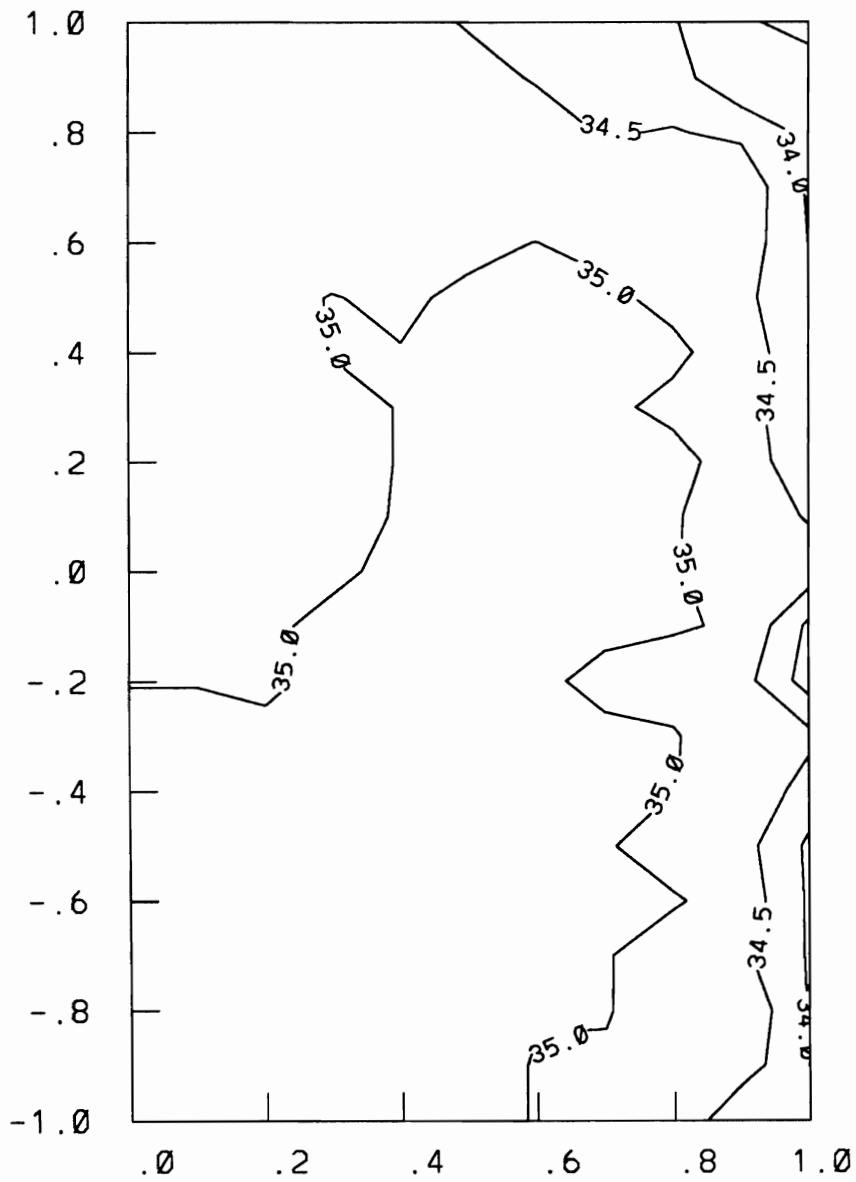


Figure 4. The upper ocean salinity field as produced by the model.
Contour interval is 0.5.

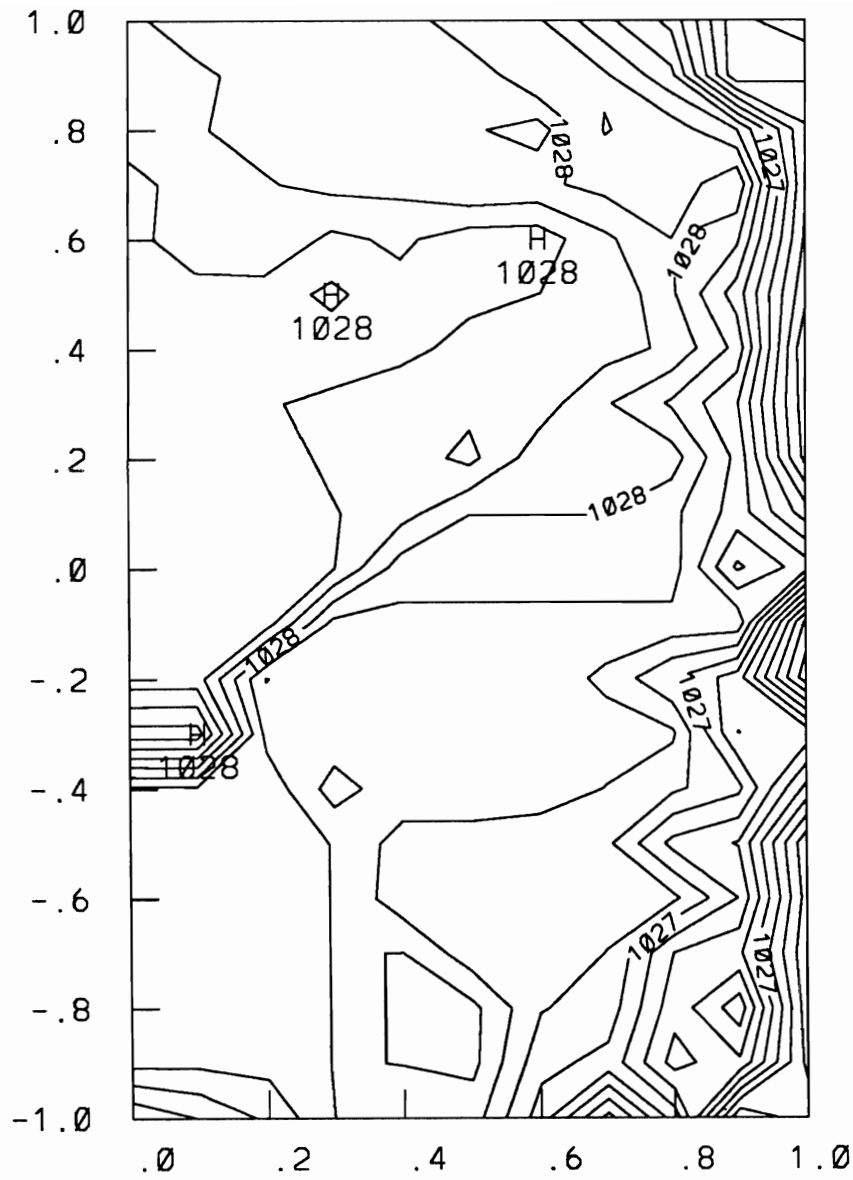


Figure 5. The upper ocean density field of the region produced using the model's temperature and salinity fields. Contour interval is 0.25.

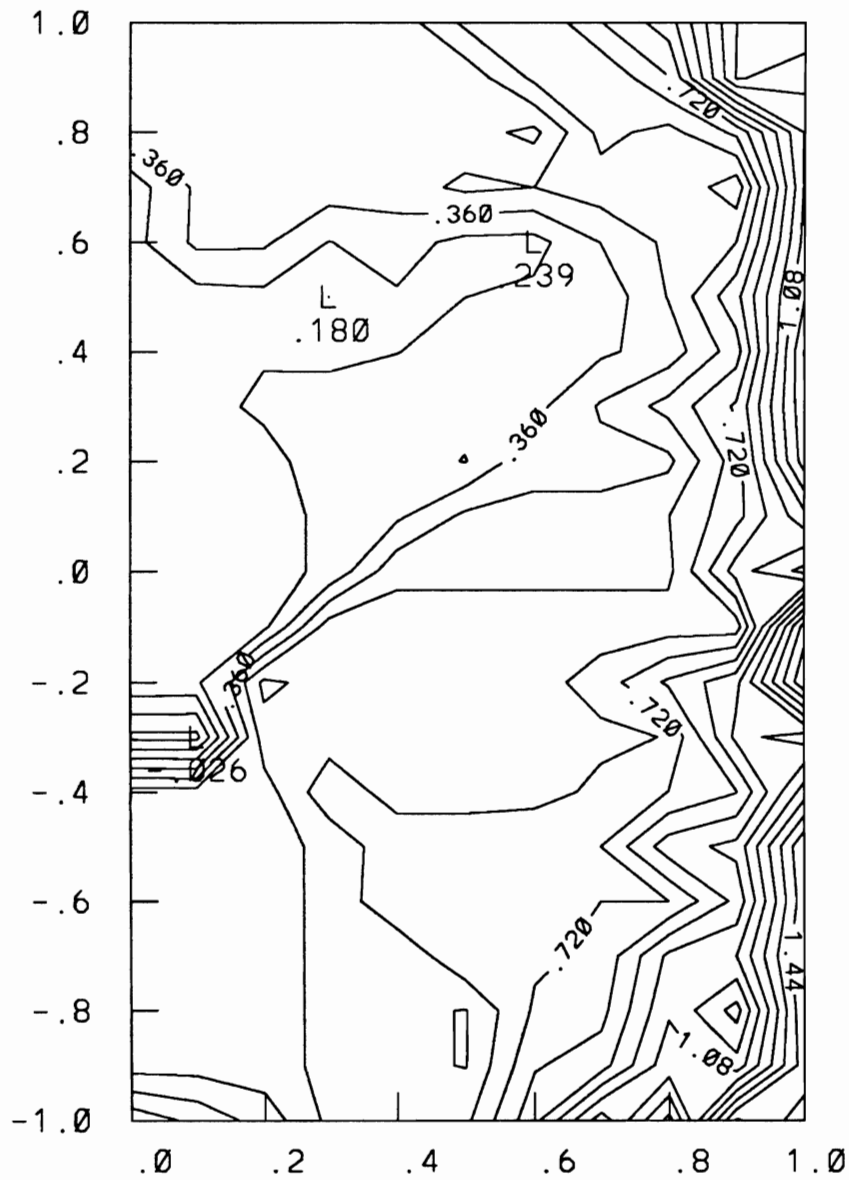


figure 6. Density difference between the fixed lower level density field ($\rho_0 = 1028 \text{ kg m}^{-3}$) and the predicted upper level density, as shown in figure 5. Contour interval is 0.09.